Research Article

A Study on the Influence of Functionalized Graphene on the Mechanical and Biocompatibility Performance of Electrospun Polyvinyl Alcohol Nanocomposites

Mogana Priya Chinnasamy
School of Mechanical Engineering, Vellore Institute of Technology, Chennai Campus, Chennai, Tamil Nadu, India

Gobinath Velu Kaliyannan
Department of Mechatronics Engineering, Kongu Engineering College, Erode, Tamil Nadu, India

Rajasekar Rathanasamy*, Sivachalapathi Senthamarai Kannan, Sreerahulraja Rajamani and Sanjith Murugesan
Department of Mechanical Engineering, Kongu Engineering College, Erode, Tamil Nadu, India

Dinesh Dhanabalan
Department of Mechanical Engineering, Bannari Amman Institute of Technology, Erode, Tamil Nadu, India

Prakash Thangaraj
Department of Physics, Builders Engineering College, Kan Geyam, Tamil Nadu, India

Saravana Kumar Jaganathan
School of Engineering, University of Lincoln, Lincoln LN6 7TS, United Kingdom

* Corresponding author. E-mail: rajasekar.cr@gmail.com DOI: 10.14416/j.asep.2024.09.007
Received: 4 May 2024; Revised: 12 July 2024; Accepted: 21 August 2024; Published online: 10 September 2024

Abstract
Polyvinyl alcohol (PVA), a synthetic polymer produced by polymerizing vinyl acetate and subjecting it to alkaline hydrolysis, exhibits properties such as film formation, emulsification, and adhesion. However, pure PVA's biocompatibility and mechanical properties are limited. Its hydrophilicity also causes it to dissolve in water and blood, rendering it less suitable for drug delivery applications. To address these limitations, PVA was crosslinked with glutaraldehyde (GA) to enhance toughness and resistance to water and blood dissolution. Additionally, carboxyl (COOH) and hydroxyl (OH) functionalized graphene were incorporated into electrospun PVA nanocomposites to further improve their mechanical properties. The results show that adding COOH- and OH-functionalized graphene in four different concentrations (0.5, 1.0, 1.5, and 2.0 wt.%) significantly enhanced the mechanical characteristics of PVA nanocomposites. Tensile strength and Young's modulus increased substantially, with OH-functionalized graphene increasing tensile strength and Young's modulus by 224% and 338.3%, respectively, and COOH-functionalized graphene increasing these properties by 245.6% and 371.4%. Morphological characterization using FT-IR and FESEM confirmed the successful incorporation of graphene into the PVA matrix. Biocompatibility testing through APTT and PT assays showed both nanocomposites are biocompatible, suggesting their potential for biomedical applications. The optimal filler concentration for both graphene types was 1.5 wt.%. This research demonstrates the promising potential of innovative materials for healthcare and biomedical engineering applications.

Keywords: Biomedical applications, Carboxyl functionalized graphene, Hydroxyl functionalized graphene, Polyvinyl alcohol

1 Introduction

Polyvinyl alcohol (PVA), a synthetic polymer famous for its versatility, has emerged as a pivotal material across diverse industries. Its biocompatibility, water solubility, and film-forming attributes have made it a cornerstone in applications ranging from textiles to adhesives and coatings [1]. In recent years, the spotlight on PVA has intensified within the biomedical realm due to its remarkable biocompatibility, positioning it as a preferred choice for applications in medicine and pharmacology. The unique properties of PVA, including non-toxicity and the ability to take various forms, such as films, hydrogels, and nanoparticles, make it a fundamental material for direct interactions with living organisms [2]–[7]. To further enhance PVA's potential for bio applications, the integration of nanoparticles, particularly COOH-functionalized graphene and OH-functionalized graphene, has proven transformative. Surface functionalization plays a pivotal role in augmenting PVA's biocompatibility, with carboxylic acid (COOH) groups ensuring superior dispersion within PVA matrices, leading to heightened interactions with biological entities. On the other hand, the inclusion of hydroxyl (OH) groups in OH-graphene enhances compatibility with water, mirroring the hydrophilic nature of biological tissues and promoting enhanced cell adhesion and overall biocompatibility [8]. In-depth technical examinations concentrating on the mechanical and biocompatible features indicate notable enhancements in both tensile strength and Young's modulus. These improvements broaden the potential applications of PVA nanocomposites, particularly in scenarios demanding load-bearing capabilities. Additionally, these nanocomposites substantiate cell adhesion and survival, illustrating their potential in tissue engineering and biomedical applications [9]–[11]. The integration of COOH- and OH-functionalized graphene into PVA nanocomposites holds promise in addressing drawbacks associated with PVA in biological and medical applications [12]–[14]. COOH-graphene enhances mechanical strength, suitable for applications like tissue engineering, while OH-graphene prioritizes biocompatibility and cell adhesion [15]. The study aims to comprehensively assess the impact of these modifications on properties such as mechanical strength and biocompatibility. The hydrophilic nature of PVA, a limitation in drug delivery systems, can be mitigated by adding graphene with distinct functional groups. This strategic approach seeks to improve PVA nanocomposite performance in critical biomedical settings. The novelty of this study lies in the first comprehensive comparison of COOH- and OH-functionalized graphene in PVA nanocomposites, demonstrating their distinct impacts on mechanical strength and biocompatibility. Utilizing the electrospinning method, we achieved enhanced structural and morphological properties, making the nanocomposites suitable for load-bearing and biomedical applications.

In this present investigation, we conducted a comparative analysis between graphene functionalized with COOH and OH groups using the electrospinning method. This cost-effective and efficient technique was employed to fabricate nanofibers, enhancing the structural, morphological, and mechanical properties of polyvinyl alcohol (PVA). The novelty of our study lies in the comprehensive comparison of COOH and OH functionalized graphene, with a specific emphasis on their mechanical and biocompatible applications. To the best of our knowledge, this marks the first instance of such an exhaustive analysis. From the conducted study, the suggestion is that nanocomposites incorporating COOH functionalized graphene demonstrated superior performance in terms of structural, morphological, and mechanical properties. We employed Fourier-transform infrared (FT-IR) spectroscopy, field emission scanning electron microscopy (FESEM), tensile testing, and coagulation assays to analyze the nanocomposite films. The detailed sample codes and descriptions are provided in Table 1.

2 Materials and Methods

2.1 *Materials*

The Polyvinyl Alcohol (PVA) (99+% hydrolyzed, MW 40,000 Da), silicone gel, and glutaraldehyde (GA) were purchased from Padma Traders Private Limited, Coimbatore, India. Functionalized graphene powder (carboxyl and hydroxyl groups) was supplied from Kongu Engineering College, Perundurai, Erode.

2.2 *Preparations of electrospinning solution*

To prepare a 10% PVA solution, initiate the process by dissolving precisely 50.0 grams of PVA in 500 mL of distilled water. The dissolution procedure should be

meticulously conducted with continuous stirring and heating the liquid to 80 °C until complete dissolution is achieved, typically taking approximately 2 h. Once the PVA is fully dissolved, allow the solution to cool. Following the cooling phase, perform a 5-minute sonication process to eliminate any bubbles present. After sonication, introduce functionalized graphene powder into the PVA solution. To ensure a well-dispersed amalgamation, employ a magnetic stirrer and maintain the solution at 60 °C in an oil bath for a duration of 24 h. This extended dispersion period facilitates the uniform distribution of functionalized graphene throughout the PVA solution, yielding a homogeneous and stable nanocomposite material suitable for diverse applications, particularly in the realm of advanced materials and composites [16], [17].

Table 1: Sample code and composition of PVA, COOH and OH functionalized graphene nanocomposites.

Sample Code	PVA (wt.%)	COOH-graphene (wt.%)	OH-graphene (wt.%)
PVA	100	-	-
PCG1	99.5	0.5	-
PCG2	99	1.0	-
PCG3	98.5	1.5	-
PCG4	98	2.0	-
PHG1	99.5	-	0.5
PHG2	99	-	1.0
PHG3	98.5	-	1.5
PHG4	98	-	2.0

2.3 *Electrospinning of nanofibers*

The electrospinning process was conducted at room temperature using a flat plate collector coated with aluminium foil. The surface of the foil was specifically treated with a silicone gel coating, enabling the easy removal of the resulting nanofiber sheets. The electrospinning setup was precise, featuring a 5 mL syringe equipped with a 23-gauge blunt-tip needle, securely connected to a voltage supply adjusted within the range of 10 to 19 kV. To maintain consistency, a precise 130 mm needle-to-collector distance was meticulously upheld, along with a constant flow rate of the PVA solution set at 0.5 mL/h [18]. It is noteworthy that the conductivity of functionalized graphene played a crucial role in influencing the stability of the spinning jet behavior during this process. This component could potentially contribute to variations in fiber diameter or the formation of bead-like structures [19]. The outcome of this meticulous approach resulted in the creation of four distinct sets of samples, each characterized by varying weight percentages of functionalized graphene (0.5, 1.0, 1.5, and 2.0%). These sets gave rise to innovative PVA/functionalized graphene composite nanofibers [17].

2.4 *Crosslinking of nanocomposite*

Crosslinking is a crucial process involving the formation of robust bonds between nanoparticles and the surrounding material, akin to establishing an intricate network of connections on a minuscule scale. These connections play a crucial role in improving the stability and durability of the nanocomposite material. fortifying it against damage and preserving its structural integrity. Essentially, it involves reinforcing the material with imperceptible links to augment toughness and reliability. To fortify the nanofiber samples, a two-step crosslinking process was employed utilizing glutaraldehyde (GA), acetone, and a small amount of HCl. Initially, the samples, including PVA/COOH, PVA/OH, and pure PVA nanofibers, were immersed in a mixture of GA and acetone. This treatment significantly toughened the samples, rendering them resistant to dissolution in water. Each set of samples received 5 mL of this solution, and they were securely stored in sealed containers. Under normal conditions, GA vapor naturally forms, instigating a reaction among the hydroxyl groups (OH) in polyvinyl alcohol (PVA) and the aldehyde groups (CHO) in glutaraldehyde (GA). This reaction strengthens the nanofibers and prevents them from dissolving in water [20]. A diagram can illustrate this chemical reaction. Following this meticulous crosslinking process, the nanofiber samples exhibited vastly improved mechanical properties, and they became impervious to dissolution in water. This marked a significant advancement in preparing the samples for detailed analysis [21].

2.5 *Mechanical properties*

Using electrospinning to incorporate COOH and OH functionalized graphene into PVA resulted in enhanced tensile strength and Young's modulus. The addition of 0.5, 1.0, 1.5, and 2.0 wt.% OH functionalized graphene resulted in improvements of 49.6, 162.4, 224, and 208.8% in tensile strength, and 60.3, 206.2, 320.2, and 338.3% in young's modulus compared to pure PVA [22]. Likewise, the incorporation of 0.5, 1.0, 1.5, and 2.0 wt.% COOH functionalized graphene led to enhancements of 80, 184.8, 245.6, and 228% in tensile strength, and 98.9,

247.8, 371.4, and 396% in Young's modulus compared to pure PVA. Significantly, as compared to OH functionalized graphene, COOH functionalized graphene showed a more noticeable improvement in both tensile strength and Young's modulus. This difference can be attributed to the formation of double hydrogen bonds between COOH graphene and PVA, creating a stronger chemical interaction than the single hydrogen bonds formed by OH graphene embedded in PVA. However, it is important to acknowledge that as we increased the nanoparticle content, the elongation at break decreased. This reduction in elongation at break is associated with the substantial reinforcement effect, where a significant increase in strength results in a notable decrease in the material's ability to stretch before breaking [23].

2.6 *Characterization technique*

2.6.1 Tensile test

Tensile testing is a means of assessing the mechanical characteristics of materials subjected to axial loading, offering insights into parameters such as tensile strength, elastic modulus, and elongation at break. In the examination of nanocomposites, specimens were crafted and exposed to a tensile test utilizing a universal testing machine, such as the Instron apparatus. During this process, both load and displacement data were meticulously recorded to construct stress-strain curves. After curve analysis, crucial mechanical properties including tensile strength, modulus of elasticity, and elongation at break were derived. A comparative assessment was then undertaken to gauge the impact of carboxyl and hydroxyl functionalized graphene on the overall mechanical performance of the nanocomposites.

2.6.2 FTIR

FTIR, a method of detecting the absorption of infrared radiation by a substance, serves to discern functional groups within a sample through their distinct vibrational frequencies. Employing an FTIR spectrometer like PerkinElmer Spectrum Two, an analysis of the nanocomposites was conducted. In this process, diminutive samples were readied, and their spectra were documented within the mid-infrared spectrum (4000–500 cm^{-1}). To ensure precise peak identification, a background spectrum was subtracted during the examination.

2.6.3 FESEM

Utilizing a focused electron beam to achieve high-resolution images of a sample's surface morphology, FESEM stands as an imaging technique of significant prowess. For the examination of nanocomposite samples, which underwent gold coating to prevent charging, a FESEM instrument—like the CARL ZEISS Sigma with Gemini column—was employed. The imaging process involved capturing visuals at diverse magnifications to scrutinize the dispersion and distribution of functionalized graphene within the polyvinyl alcohol matrix. The assessment encompassed a thorough examination of morphological aspects, including particle size, distribution patterns, and the interfacial bonding existing between graphene and the polymer matrix.

2.6.4 Coagulation assay

Evaluating the intrinsic and extrinsic pathways of the coagulation cascade, APTT and PT serve as clotting assays. The process involves acquiring blood plasma, followed by the measurement of APTT and PT utilizing suitable reagents. Subsequently, the coagulation times are compared between nanocomposites featuring carboxyl and hydroxyl functionalized graphene to assess their respective effects on blood clotting.

3 Results and Discussions

3.1 *Fourier transform infrared spectroscopy (FT-IR)*

The analysis of carboxyl and hydroxyl-functionalized graphene nanocomposites was conducted using FT-IR spectroscopy. The findings highlight the crucial role of the C-OH stretching vibration in carboxyl graphene within the hydrogen spectra [24]. Figure. 1 presents the FT-IR spectra of polyvinyl alcohol (PVA) doped carboxyl graphene and hydroxyl graphene at varying ratios. Notably, a broad absorption peak spanning from 3306 cm^{-1} to 3315 cm^{-1} signifies -OH symmetrical stretching vibrations [25]. The peaks at 2920 cm^{-1} and 1255 cm^{-1} are associated with CH stretching and COOH/OH deformation vibrations, respectively. The absorption peak at 1735 cm^{-1} in pure PVA corresponds to the stretching vibrations of the C=O group, with intensity escalating with higher doping ratios [26]. The OH stretching vibrations peak, ranging between 3306 cm^{-1} and 3315 cm^{-1} in the

nanocomposites, undergoes a shift and increase in wavenumber with elevated doping percentages a phenomenon linked to hydrogen bond formation between PVA and graphene sheets. The nanocomposites demonstrate a noteworthy enhancement in tensile strength, elongation, and modulus of elasticity values compared to hydroxyl graphene. The absorption peak at 827 cm^{-1} is attributed to C-O-C, C-C, -OH, and C-H stretching vibrations. Finally, the peaks observed at 591 cm^{-1} to 466 cm^{-1} in the nanocomposites affirm the presence of both graphene carboxyl and graphene hydroxyl functional groups [16].

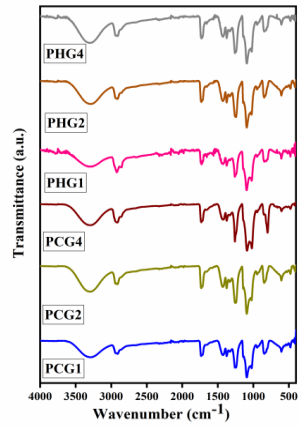

Figure 1: FT-IR spectra: PCG1, PCG2, PCG3, PCG4, PHG1, PHG2, PHG3 and PHG4 nanocomposites.

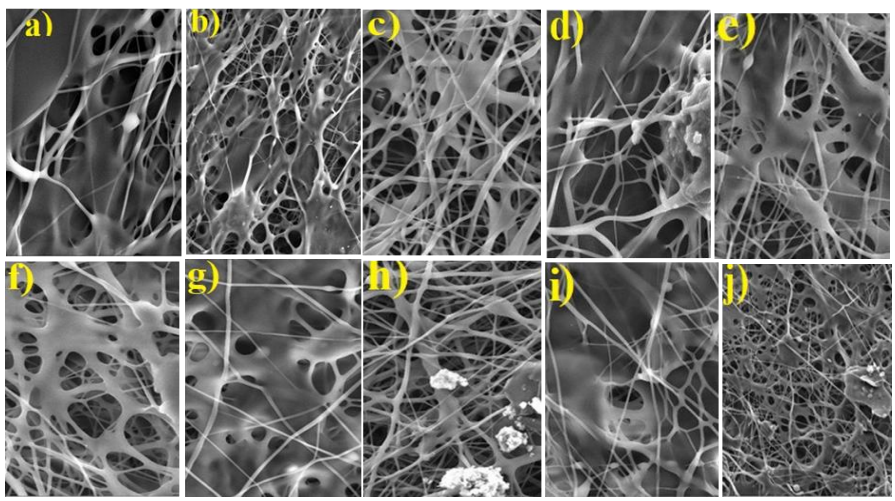

Figure 2: FE-SEM image: (a) pure PVA (uncrosslinked), (b) pure PVA (crosslinked), (c) PCG1, (d) PCG2, (e) PCG3 (f) PCG4, (g) PHG1, (h) PHG2, (i) PHG3, (j) PHG4.

3.2 *Field emission scanning electron microscope (FESEM)*

Figure 2 presents detailed insights into the structural morphology of pure PVA and its nanocomposites with COOH- and OH-functionalized graphene, as captured by field emission scanning electron microscopy (FESEM). In Figure 2(a), an intricate depiction emerges, revealing agglomerated nanofibers in the case of pure PVA, particularly in its uncrosslinked form. Upon crosslinking the pure PVA, as depicted in Figure 2(b), a noticeable transformation occurs, showcasing a more uniform and organized arrangement of agglomerated nanofibers. Moving on to Figure 2(c)–(f), a comprehensive exploration of COOH-functionalized graphene at different ratios (0.5, 1.0, 1.5, and 2.0 wt.%) unfolds. The surface morphology of COOH undergoes substantial modification as the doping percentage of carboxyl graphene increases. Notably, a significant presence of agglomerated, non-uniform nanofibers is observed, providing critical insights into the impact of varying carboxyl graphene concentrations on the nanocomposite's architecture. Figure 2(g)–(j) extends this analysis to OH-functionalized graphene with analogous weight percentages. The surface morphology of OH is dynamically altered with an increase in the doping percentage of hydroxyl graphene. Intriguingly, a drastic modification is observed, featuring uniform, non-agglomerated

nanofibers when the highest ratio of hydroxyl graphene is introduced. This observation sheds light on the nuanced relationship between the doping percentage of hydroxyl graphene and the resulting nanofiber arrangement, offering valuable information for applications requiring precise control over structural characteristics.

3.3 *Mechanical properties*

3.3.1 Tensile strength

The tensile test was done using universal testing equipment and the change in tensile strength was recorded with a relevant sample. Figure 3 displays the tensile strength vs sample code of the PVA composite. Each bar indicates the tensile strength demonstrated by the sample. Figure 3, The PVA nanocomposite exhibits a notable improvement in tensile strength up to 1.5 wt.% of COOH graphene addition, with a high of 43.2 MPa being reached. In contrast, the tensile strength of the PVA nanocomposite with 1.5 wt.% of OH graphene addition is only 40.1 MPa [27]. This suggests that COOH functional groups are more effective than OH functional groups in improving the tensile strength of PVA nanocomposites. An increase in the addition of nanoparticle leads to the agglomeration of particulates in the PVA matrix. This proves that 1.5 wt.% of graphene is the optimal content that forms uniform distribution in the PVA matrix [28].

3.3.2 Elongation at break

The elongation at break percentage for pure PVA nanocomposites, PVA/functionalized graphene nanocomposite can be graphically represented, and a good trend is observed when graphene is added, resulting in a reduction in elongation at break. This is attributed to the extent of reinforcement effect, where a strong reinforcement effect leads to a significant drop in elongation at break. Figure 4, it is evident that the elongation at break decreases significantly up to a 2.0 wt.% graphene addition. This reduction transitions from 105% of the pure PVA value to 69% when COOH-functionalized graphene is incorporated into the PVA composite. This observation underscores the positive impact of adding graphene to the PVA composite [29]. It can be attributed to a strong reinforcement effect, resulting in a significant reduction in the elongation at break, which is indicative of improved material strength.

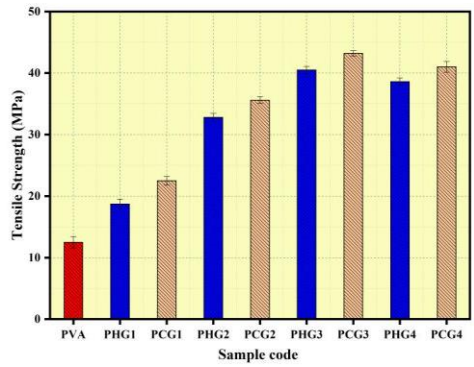

Figure 3: Tensile strength for electrospun PVA nanocomposite.

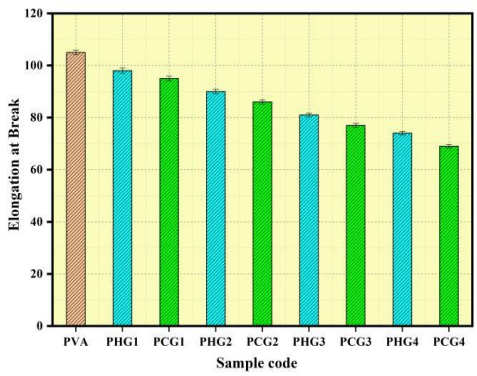

Figure 4: Elongation at break for electrospun PVA nanocomposite.

3.3.3 Modulus of elasticity

The modulus of elasticity for pure PVA, PVA/functionalized graphene nanocomposites can be graphically represented, and a good trend is observed when graphene is added, resulting in a significant rise in modulus of elasticity. This due to the carbon-carbon bonds in graphene are incredibly strong and covalent, which means the atoms share electrons very efficiently. This results in an extremely stiff and stable structure, giving graphene its remarkable modulus of elasticity. Figure 5 shows that the modulus of elasticity for the PVA nanocomposite experiences a significant increase, reaching a peak value of 59.02 MPa with the incorporation of 2.0 wt.% COOH-functionalized graphene. In contrast, the modulus of elasticity for the PVA nanocomposite with 2.0 wt.% OH-functionalized graphene addition is notably lower, at 52.16 MPa. These findings suggest that the COOH functional groups exhibit greater effectiveness than the OH functional groups in influencing the modulus of elasticity behavior in the nanocomposite.

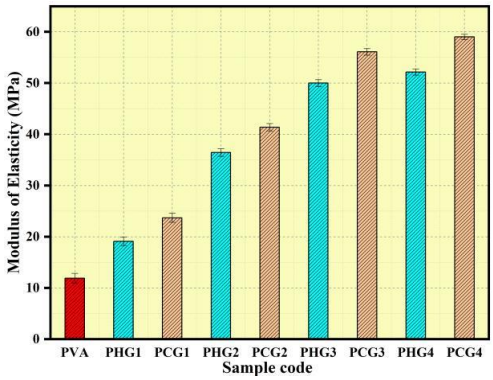

Figure 5: Modulus of elasticity for electrospun PVA nanocomposite.

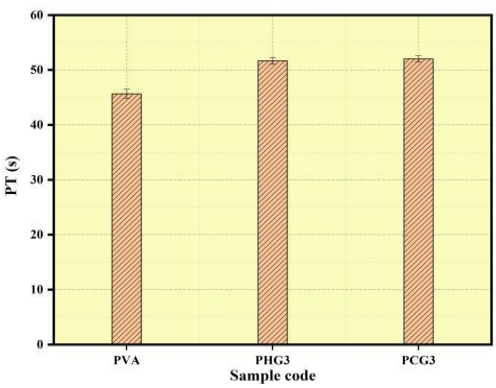

Figure 6: Prothrombin time values for nanocomposites sample of PVA, PHG3 and PCG3.

3.4 *Coagulation assay*

Blood coagulation assays were conducted on electrospun PVA, PVA/COOH graphene, and PVA/OH graphene samples after a crosslinking procedure. A specific amount of platelet-poor plasma (PPP) was applied to the sample surfaces, and coagulation agents were added to measure prothrombin time (PT) and activated partial thromboplastin time (APTT). The coagulation assays showed that the APTT values of the developed composites were significantly higher than those of pure PVA. The prolonged coagulation time can be attributed to the additional functional groups in the composite. These functional groups may interact with platelets and other coagulation factors in a way that delays the coagulation process. Delayed coagulation could be advantageous for wound healing applications [30].

When a wound occurs, platelets are activated and aggregate to form a clot. This clot helps to stop the bleeding and provides a scaffold for new tissue growth. However, if the coagulation process is too rapid, it can lead to the formation of a dense clot that can impede wound healing. By prolonging coagulation, functionalized PVA composites may help to promote wound healing by allowing for more time for platelets to aggregate and form a loose, porous clot. However, it is important to note that delayed coagulation could also have negative consequences. For example, if coagulation is delayed too long, it could lead to excessive bleeding. Additionally, delayed coagulation could increase the risk of infection, as it would allow more time for bacteria to enter the wound. Therefore, it is important to carefully evaluate the potential benefits and risks of using functionalized PVA composites for wound healing applications. Further research is needed to investigate the effects of these materials on platelet adhesion, complement activation, and other aspects of the coagulation cascade.

Prothrombin, a protein synthesized by the liver, is among the myriad factors within the bloodstream responsible for facilitating proper coagulation. When a Prothrombin Time (PT) test indicates that blood takes longer to clot compared to the reference range, this delayed coagulation may offer potential benefits, particularly in the context of wound healing and severe injuries. Table 2 shows the APTT and PT values of the nanocomposite samples.

Table 2: APTT and PT values of the nanocomposite samples.

Sample Codes	APTT(s)	PT(s)
PVA	160.6	45.6
PCG3	171.3	51.6
PHG3	171.6	52

Figure 6 The study analyzed the prothrombin time consumption of PVA nanocomposites with different graphene additives, PHG3 and PCG3. The higher the PT, the better the blood clotting ability, which is beneficial for biomedical wound healing applications. PCG3 (52s) had a higher PT than PHG3 (51.6 s), likely due to its interaction with positively charged blood platelets. This suggests that PCG3 is a more promising material for biomedical wound healing than PHG3. The Activated partial thromboplastin time (APTT) for blood samples when coagulation agents were added to the PVA, PVA/COOH graphene, and PVA/OH graphene nanocomposite samples Figure 7. The graph demonstrates the impact of adding OH graphene (PHG3) and COOH graphene (PCG3) to PVA nanocomposites on APTT, a measure of blood clotting

time. Both PHG3 and PCG3 reduce APTT, but PCG3 is more effective due to its hydrophilic nature, which interacts more strongly with water molecules, creating a more hydrated environment conducive to blood clotting. Lower APTT is generally better for biomedical wound healing applications.

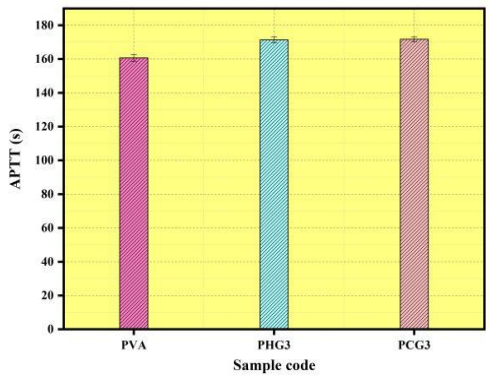

Figure 7: Activated partial thromboplastin time value for nanocomposite samples of PVA, PHG3 and PCG3.

4 Conclusions

The study explores the mechanical and biocompatibility performance of carboxyl (COOH) and hydroxyl (OH) functionalized graphene embedded in electrospun polyvinyl alcohol (PVA) nanocomposites. The incorporation of OH-functionalized graphene and COOH-functionalized graphene into pure PVA resulted in significant enhancements in both tensile strength and Young's modulus. Specifically, OH-functionalized graphene led to a remarkable increase of 224% in tensile strength and 338.3% in Young's modulus compared to pure PVA. Similarly, COOH-functionalized graphene exhibited notable improvements, elevating tensile strength by 245.6% and Young's modulus by 371.4%. Because this enhancement comes with a loss in elongation at the breaking point, strength and flexibility may have to be traded off. The biocompatibility of these nanocomposites was assessed through activated partial thromboplastin time (APTT) and prothrombin time (PT) tests, indicating their good biocompatibility, and suggesting potential use in biomedical applications. The study highlights the potential for the development of advanced materials with diverse applications in healthcare and biomedical engineering. Further research and optimization of these nanocomposites may lead to the creation of novel materials with tailored mechanical and biocompatible properties.

Acknowledgments

Authors thank Kongu Engineering College and Bannari Amman Institute of Technology for providing Research Facilities.

Author Contributions

R.R.: conceptualization, investigation, G.V.K.: reviewing and editing; M.C.: methodology, investigation, S.S.K.: writing an original draft; S.R.: research design, data analysis; S.M.: conceptualization, D.D.: data curation, P.T.: writing-reviewing and editing, S.K.J.: validation and visualization. All authors have read and agreed to the published version of the manuscript.

Conflicts of Interest

The authors declare no conflict of interest.

References

[1] S. K. Palaniappan, M. K. Singh, S. M. Rangappa, and S. Siengchin, "Eco-friendly biocomposites: A step towards achieving sustainable development goals," *Composites*, vol. 7, pp. 1–3, 2023.

[2] J. Chen, Y. Li, Y. Zhang, and Y. Zhu, "Preparation and characterization of graphene oxide reinforced PVA film with boric acid as crosslinker," *Journal of Applied Polymer Science*, vol. 132, no. 22, 2015, doi: 10.1002/app.42000.

[3] J. Jose, M. A. Al-Harthi, M. A. A. AlMa'adeed, J. B. Dakua, and S. K. De, "Effect of graphene loading on thermomechanical properties of poly (vinyl alcohol)/starch blend," *Journal of Applied Polymer Science*, vol. 132, no. 16, 2015, doi: 10.1002/app.41827.

[4] R. Surudzic, A. Jankovic, M. Mitric, I. Matic, Z. D. Juranic, L. Zivkovic, V. Miskovic-Stankovic, K. Y. Rhee, S. J. Park, and D. Hui, "The effect of graphene loading on mechanical, thermal and biological properties of poly (vinyl alcohol)/ graphene nanocomposites," *Journal of Industrial and Engineering Chemistry*, vol. 34, pp. 250–257, 2016.

[5] J. Wang, X. Wang, C. Xu, M. Zhang, and X. Shang, "Preparation of graphene/poly (vinyl alcohol) nanocomposites with enhanced mechanical

properties and water resistance," *Polymer International*, vol. 60, pp. 816–822, 2011.

[6] N. Georgieva, R. Bryaskova, and R. Tzoneva, "New Polyvinyl alcohol-based hybrid materials for biomedical application," *Materials Letters*, vol. 88, pp. 19–22, 2012.

[7] R. Phiri, S. M. Rangappa, S. Siengchin, and D. Marinkovic, "Agro-waste natural fiber sample preparation techniques for bio-composites development: Methodological insights," *Facta Universitatis, Series: Mechanical Engineering*, vol. 21, pp. 631–656, 2023.

[8] R. Eivazzadeh-Keihan, F. Radinekiyan, H. Madanchi, H. A. M. Aliabadi, and A. Maleki, "Graphene oxide/alginate/silk fibroin composite as a novel bionanostructure with improved blood compatibility, less toxicity and enhanced mechanical properties," *Carbohydrate Polymers*, vol. 248, 2020, Art. no. 116802.

[9] M. A. Kanjwal and A. A. Ghaferi, "Graphene incorporated electrospun nanofiber for electrochemical sensing and biomedical applications: A critical review," *Sensors*, vol. 22, p. 8661, 2022.

[10] D. Nataraj, R. Reddy, and N. Reddy, "Crosslinking electrospun poly (vinyl) alcohol fibers with citric acid to impart aqueous stability for medical applications," *European Polymer Journal*, vol. 124, 2020, Art. no. 109484.

[11] J. W. Drexler and H. M. Powell, "Dehydrothermal crosslinking of electrospun collagen," *Tissue Engineering Part C: Methods*, vol. 17, pp. 9–17, 2011.

[12] X. Li, X. Yang, Z. Wang, Y. Liu, J. Guo, Y. Zhu, J. Shao, J. Li, L. Wang, and K. Wang, "Antibacterial, antioxidant and biocompatible nanosized quercetin-PVA xerogel films for wound dressing," *Colloids and Surfaces B: Biointerfaces,* vol. 209, 2022, Art. no. 112175.

[13] R. Gobi, P. Ravichandiran, R. S. Babu, and D. J. Yoo, "Biopolymer and synthetic polymer-based nanocomposites in wound dressing applications: A review," *Polymers*, vol. 13, p. 1962, 2021.

[14] I. Suyambulingam, S. M. Rangappa, and S. Siengchin, "Advanced materials and technologies for engineering applications," *Applied Science and Engineering Progress*, vol. 16, pp. 6760–6760, 2023.

[15] M. Koosha and H. Mirzadeh, "Electrospinning, mechanical properties, and cell behavior study of chitosan/PVA nanofibers," *Journal of Biomedical Materials Research Part A*, vol. 103, pp. 3081–3093, 2015.

[16] M. Aslam, M. A. Kalyar, and Z. A. Raza, "Fabrication of reduced graphene oxide nanosheets doped PVA composite films for tailoring their opto-mechanical properties," *Applied Physics A*, vol. 123, pp. 1–12, 2017.

[17] F. H. Falqi, O. A. Bin-Dahman, M. Hussain, and M. A. Al-Harthi, "Preparation of miscible PVA/PEG blends and effect of graphene concentration on thermal, crystallization, morphological, and mechanical properties of PVA/PEG (10 wt%) blend," *International Journal of Polymer Science*, vol. 2018, no. 1, 2018, Art. no. 852793.

[18] H. Adeli, M. T. Khorasani, and M. Parvazinia, "Wound dressing based on electrospun PVA/chitosan/starch nanofibrous mats: Fabrication, antibacterial and cytocompatibility evaluation and in vitro healing assay," *International Journal of Biological Macromolecules*, vol. 122, pp. 238–254, 2019.

[19] Y.-H. Chien, M.-T. Ho, C.-H. Feng, J.-H. Yen, Y.-C. Chang, C.-S. Lai, and R.-F. Louh, "Fabrication of glutaraldehyde vapor treated PVA/SA/GO/ZnO electrospun nanofibers with high liquid absorbability for antimicrobial of *Staphylococcus aureus*," *Nanomaterials*, vol. 13, p. 932, 2023.

[20] C. Tang, C. D. Saquing, J. R. Harding, and S. A. Khan, "In situ cross-linking of electrospun poly (vinyl alcohol) nanofibers," *Macromolecules*, vol. 43, pp. 630–637, 2010.

[21] H. Tian, L. Yuan, J. Wang, H. Wu, H. Wang, A. Xiang, B. Ashok, and A. V. Rajulu, "Electrospinning of polyvinyl alcohol into crosslinked nanofibers: An approach to fabricate functional adsorbent for heavy metals," *Journal of hazardous Materials*, vol. 378, 2019, Art. no. 120751.

[22] Y.-s. Jun, S. Habibpour, M. Hamidinejad, M. G. Park, W. Ahn, A. Yu, and C. B. Park, "Enhanced electrical and mechanical properties of graphene nano-ribbon/thermoplastic polyurethane composites," *Carbon*, vol. 174, pp. 305–316, 2021.

[23] A. A. Iqbal, N. Sakib, A. P. Iqbal, and D. M. Nuruzzaman, "Graphene-based nanocomposites and their fabrication, mechanical properties and applications," *Materialia*, vol. 12, 2020, Art. no. 100815.

[24] X. Yang, L. Li, S. Shang, and X.-m. Tao, "Synthesis and characterization of layer-aligned

poly (vinyl alcohol)/graphene nanocomposites," *Polymer*, vol. 51, pp. 3431–3435, 2010.

[25] S. Gahlot, P. P. Sharma, V. Kulshrestha, and P. K. Jha, "SGO/SPES-based highly conducting polymer electrolyte membranes for fuel cell application," *ACS Applied Materials and Interfaces*, vol. 6, pp. 5595–5601, 2014.

[26] C. Bao, Y. Guo, L. Song, and Y. Hu, "Poly (vinyl alcohol) nanocomposites based on graphene and graphite oxide: A comparative investigation of property and mechanism," *Journal of Materials Chemistry*, vol. 21, pp. 13942–13950, 2011.

[27] H. K. F. Cheng, N. G. Sahoo, Y. P. Tan, Y. Pan, H. Bao, L. Li, S. H. Chan, and J. Zhao, "Poly (vinyl alcohol) nanocomposites filled with poly (vinyl alcohol)-grafted graphene oxide," *ACS applied materials and Interfaces*, vol. 4, pp. 2387–2394, 2012.

[28] T. Cheng-an, Z. Hao, W. Fang, Z. Hui, Z. Xiaorong, and W. Jianfang, "Mechanical properties of graphene oxide/polyvinyl alcohol composite film," *Polymers and Polymer Composites*, vol. 25, pp. 11–16, 2017.

[29] Y. Wang, G. Yang, W. Wang, S. Zhu, L. Guo, Z. Zhang, and P. Li, "Effects of different functional groups in graphene nanofiber on the mechanical property of polyvinyl alcohol composites by the molecular dynamic simulations," *Journal of Molecular Liquids*, vol. 277, pp. 261–268, 2019.

[30] S. K. Jaganathan and M. P. Mani, "Electrospun polyurethane nanofibrous composite impregnated with metallic copper for wound-healing application," *3 Biotech*, vol. 8, p. 327, 2018.